Journal of Colloid and Interface Science 490 (2017) 452–461

Contents lists available at ScienceDirect

Journal of Colloid and Interface Science

journal homepage: www.elsevier.com/locate/jcis

Regular Article

Biopolymer matrix for nano-encapsulation of urease – A model protein and its application in urea detection

Abhishek Saxena [a], Arpita Bhattacharya [b], Satish Kumar [c], Irving R. Epstein [d], Rachana Sahney [a,*]

[a] Amity Institute of Biotechnology, AUUP, Noida 201301, India
[b] Amity Institute of Nanotechnology, AUUP, Noida 201301, India
[c] St. Stephens College, Delhi University, New Delhi 110007, India
[d] Department of Chemistry, Brandeis University, 415 South Street, MS 015, Waltham, MA 02453, United States

GRAPHICAL ABSTRACT

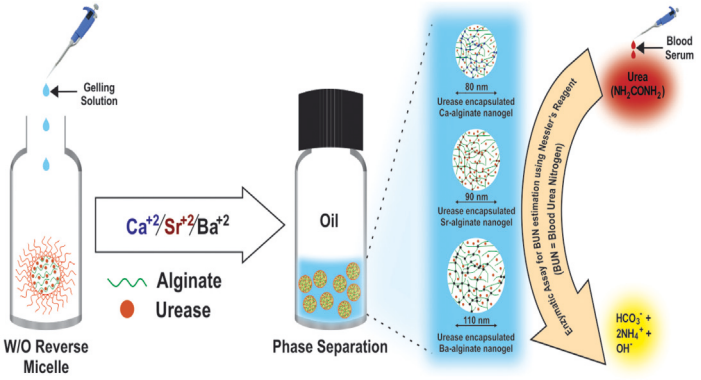

ARTICLE INFO

Article history:
Received 7 September 2016
Revised 7 November 2016
Accepted 8 November 2016
Available online 9 November 2016

Keywords:
Nanoparticles
W/O nanoemulsions
Urease
Alginate nanogels

ABSTRACT

Alginate microparticles and nanoparticles crosslinked with Ca^{+2} ions are frequently employed in biomedical applications. Here we use microemulsion polymerization to prepare alginate nanoparticles (nanogels) using different crosslinking ions (Ca^{+2}, Sr^{+2}, Ba^{+2}) to encapsulate a model protein, urease enzyme (jackbeans). With alginate concentrations of 0.2 wt% in the aqueous phase, emulsion droplets showed good stability and narrow, monomodal distributions with radii ~65 ± 10 nm. The size of the nanogel varies with the crosslinking cation and its affinity for the mannuronate and guluronate units in the linear alginate chain. The nanogels were further characterized using dynamic light scattering, scanning electron microscopy, energy dispersive X-ray spectrometry and zeta potential. This work demonstrates the potential application of Ba-alginate as an alternative matrix for nano-encapsulation of proteins and its use for biomedical applications.

1. Introduction

Alginate is a linear biopolymer obtained from brown algae. It contains β-d-mannuronate (M) and α-l-guluronate (G) residues linearly linked by 1,4-glycosidic linkages in varying proportions, sequences, and molecular weights [1]. The notable biomedical

* Corresponding author at: Amity Institute of Biotechnology, Amity University Uttar Pradesh, Noida 201301, UP, India.
E-mail addresses: satish@ststephens.edu (S. Kumar), epstein@brandeis.edu (I.R. Epstein), rsahney@amity.edu (R. Sahney).

http://dx.doi.org/10.1016/j.jcis.2016.11.030
0021-9797/

applications of natural polysaccharides in wound dressings [2], cell encapsulation [3–5], drug delivery [6], catalyst support [7], and biosensors [8,9] result from the ease of forming heat-stable gels by ionic cross-linking with multivalent cations, user-friendly preparation methods, the possibility to encapsulate various sensitive molecules (synthetic or biomolecules), and the robustness of production under ambient physiological conditions [10]. The preparation, properties and application of calcium alginate microgels are well documented [11], but stability studies on calcium alginate microgel particles indicate a number of drawbacks, such as instability in physiological liquids [12] and poor thermal stability, as well as fractures and cavities (in homogeneous porous networks) and poor mechanical resistance due to decreasing gel strength from the surface to the core [13,14]. These microgels cannot be used for immobilization of biomolecules with molecular weights less than 300 kDa due to high leakage of biomolecules [15]. Thus, low mechanical strength of the gel structure and serious swelling properties greatly limit applications. Many literature reports describe the biological application of Ba-alginate microbeads, which are effective in a variety of applications [3–5]. Thus, in addition to calcium, other divalent cations are candidates as crosslinks for the development of more suitable alginate gels for different applications.

The use of alginate in nanoparticles (nanogels) is less common than that of synthetic polymers like poly(lactic acid) (PLA), poly (glycolic acid) (PGA) and poly(lactide-co-glycolide) (PLGA). Preparation of Ca-alginate nanogels for the development of nano-sized drug delivery systems has been reported [6,11], largely based on two methods [16]: (a) Complexation, where nanoparticles can be prepared by self-assembly and complexing alginate with highly charged polycations, such as chitosan or poly l-lysine [17]. The inclusion of polycations, however, limits versatility. Yu et al. [18] have reported nanosized aggregates with four different morphologies, nanosphere, vesicle, nanoparticle and nanorod, prepared under very mild conditions through self-assembly of alginate polymer with Ca^{+2} cations, a process that requires almost a week to obtain calcium alginate nanogels. However, solid nanoparticles could not be obtained through this method. (b) Alginate-in-oil (W/O) emulsion systems have been used to entrap water-insoluble drug entities in calcium alginate nanoparticles, where development of nanoemulsions requires a large input of mechanical energy. Shearing, ultrasonication and solvent exchange procedures have been employed to attain a sufficient increase in the surface-to-volume ratio [19]. However, such harsh treatment may seriously damage sensitive biomacromolecules like enzymes or antibodies in comparison to milder methods. The latter, however, produce particle sizes above the desired range as well as high polydispersity [20]. Recently, Machado et al. [21] proposed a phase inversion temperature (PIT) emulsification technique, but this is unsuitable for encapsulation of temperature-sensitive biomolecules like proteins.

We use urease enzyme as a model protein to study the widely used sol-gel emulsification polymerization method of protein encapsulation, as it gives a highly selective response to the biologically important molecule urea, which is of great interest (i) in clinical diagnosis, since it is the primary reliable index of renal function [22]; (ii) in environmental analysis, since it is used as a nitrogenous fertilizer that causes environmental stress [23]; and (iii) in the detection of adulteration in dairy milk or in assessing the nutritional program of lactating dairy cows [24]. Urease enzyme-based analytical systems are used for the monitoring of urea in these fields when the critical issue is maintaining the stability, activity, and function of the enzyme as close as possible to its native state [25]. The application of immobilized enzymes is preferred due to their ease of handling, prolonged availability, robustness, increased resistance to environmental changes and reusability [26]. The characteristics of immobilized enzymes are controlled by the properties of both the enzyme and the support matrix. The present study is designed to prepare alginate nanogels using various divalent ions- (Ca^{+2}, Ba^{+2} and Sr^{+2}) -as crosslinks and to compare the effects of these crosslinks on the morphology, surface charge, protein encapsulation properties and stability of the resulting nanogels. The success of urease immobilization was determined by the study of various immobilization parameters, *i.e.*, enzyme loading and specific enzyme activity over a period of four weeks. We further studied the application of encapsulated urease for urea measurement in clinical blood serum samples and compared the results with the those obtained from the recommended clinical method of blood urea nitrogen (BUN) analysis using an auto analyser.

2. Experimental

2.1. Materials

Sodium alginate (mol. wt. 120,000–190,000), urease and hexane were purchased from Sigma-Aldrich. Polyoxyethylene sorbitan mono-oleate (Tween 80), calcium chloride dihydrate ($CaCl_2{\cdot}2H_2O$, p.a.), sodium chloride, Nessler's reagent and urea were supplied by Fisher Scientific. Other chemicals like strontium chloride, barium chloride, Tris-acetate and sodium acetate were obtained from Qualigens India. All chemicals were used as received. Double-distilled water was used throughout the experiments.

2.2. Preparation of alginate nanoparticles (alginate nanogels) using $Ca^{+2}/Sr^{+2}/Ba^{+2}$ crosslinkers and encapsulation of urease

The sodium alginate solution (0.2%) was prepared in Tris-acetate-saline buffer (100 mM, pH 7.2) at 4 °C. This solution was added dropwise to a vial containing the organic phase (hexane = 20.44 g) and Tween 80 under constant stirring at 500 rpm. Various phases appeared (transparent to turbid) during the process of adding alginate solution at different surfactant concentrations. For each distinct phase, the mixture was further stirred for 30 min, and 10 mL of filtered solutions containing divalent cations ($CaCl_2$, $BaCl_2$ or $SrCl_2$, 100 mM) were added dropwise, which led to crosslinking of the polymer chains. After careful washing with deionized water to remove surfactant and hexane, the vial was centrifuged at 3000 g for 30 min, and small white pellets of alginate nanogel were obtained. The pellets were re-suspended in Tris-acetate-saline buffer for successive studies. For the encapsulation of urease into the alginate nanogels, the procedure was same as described above except that urease was pre-mixed with the 0.2% alginate solution.

2.3. Characterization

2.3.1. Size determination using dynamic light scattering (DLS)

A 1 mL aliquot of the sample (emulsion and/or particle suspension) was placed in a quartz cuvette and analyzed using DLS to estimate the mean hydrodynamic diameter and the polydispersity index (PDI). The experiments were performed on a Malvern Zetasizer - Nano ZS (Malvern, UK) instrument with backscatter detection (173°), controlled by Dispersion Technology Software (DTS 5.03, Malvern, UK). Mean hydrodynamic radii and intensity-averaged size distributions were obtained from the raw data using the general-purpose inverse Laplace transform method provided in the instrument software. The PDIs were estimated from cumulant analysis, which is also provided with the instrument software.

2.3.2. SEM-EDX measurement

The surface morphologies (shape and formation of aggregates) and sizes of nanoparticle formulations of alginate nanoparticles were studied using scanning electron microscopy (SEM). Specimen preparation was performed as follows: the lyophilized nanogels were first suspended in ethanol. The suspension thus obtained was mounted on stubs and sputter-coated with gold. Micrographs were taken on a SEM instrument (Model S-4800 microscope, Hitachi, Tokyo, Japan). The nanogels mounted on stubs were further used to analyze the presence of metal cations by using an electron probe X-ray microanalyzer in energy dispersive X-ray spectrometry (EDX) mode.

2.3.3. FT-IR spectral study

Samples of sodium alginate, urease and encapsulated urease in various alginate nanogels cross-linked with Ca^{+2}, Sr^{+2} and Ba^{+2} were lyophilized before performing FT-IR analysis. The FT-IR spectra were recorded on a Perkin-Elmer spectrometer. The spectra were collected from 4000 to 400 cm^{-1} in the transmission mode.

2.3.4. Surface charge characteristics using zeta potential measurements

The DLS instrument Malvern Zetasizer Nano ZS (Malvern, UK) was used to measure the zeta potential in the electrophoretic light scattering (ELS) mode. The alginate nanogels containing different crosslink ions (Ca^{+2}, Sr^{+2} and Ba^{+2}) with 0.5 w/v particle concentration were suspended in water (Milli-Q) and slowly placed in a standard cell to avoid air bubbles. When the cell was inserted into the Zetasizer, electrodes positioned on either side of the cell holder supplied the voltage necessary to perform electrophoresis. The zeta potentials were calculated automatically at 25 °C by the instrument, determining the electrophoretic mobility using the Henry equation [27]. Each sample was run in triplicate, and the average of the three readings was reported.

2.4. Enzyme assay

Lyophilized urease enzyme (2 mg/mL) was premixed with sodium alginate sol (0.2%) for the encapsulation of urease protein in the nanogels using different crosslinking ions. The nanogels so obtained were washed, lyophilized and resuspended in buffer. The specific enzyme activity of immobilized enzyme and residual enzyme in the wash solution were separately determined as follows: The appropriate amount of soluble enzyme in stock solution or wash solution (0.1 mL) or immobilized urease nanogel (0.001 g) was incubated in 0.1 M urea with intermittent shaking. The amount of NH_3 liberated after incubation for a fixed time interval was determined using Nessler's reagent [28]. The absorbance was measured spectrophotometrically at 405 nm (Shimadzu UV–vis spectrophotometer, Japan). One unit of urease activity liberates 1 μmol of NH_3 from 0.1 M urea per min under standard assay conditions (100 mM Tris-acetate-saline buffer, pH 7.2 and 25 °C).

The protein content in the alginate nanogel was determined by the method of decrosslinking of alginate nanogels in brine solution given by Pignolet et al. [29]. In this method the breaking of cation-alginate crosslinks releases urease protein, which was estimated by Bradford's method [30]. The residual protein content of the wash solution was also determined by the Bradford method of protein estimation [30].

The enzyme loading efficiency and loading capacity of the nanogels were calculated as follows:

A. Enzyme loading efficiency

$$= \frac{Wt.\ of\ urease\ in\ alginate\ sol - Wt.\ of\ residual\ urease}{Wt.\ of\ urease\ in\ alginate\ sol} \times 100$$

B. Loading Capacity

$$= \frac{Wt.\ of\ urease\ in\ alginate\ sol - Wt.\ of\ residual\ urease}{Polymer\ weight}$$

The percent immobilization (percent enzyme activity retention in the alginate nanogel) was calculated as follows:

C. Percent immobilization (%)

$$= \frac{\text{Specific activity of immobilized urease}}{\text{Specific activity of soluble urease}} \times 100$$

The specific activity of immobilized urease was determined as detailed above. The specific activity of soluble urease was calculated by subtracting the specific activity of urease during washing (unbound urease) from the specific activity of total soluble enzyme.

2.5. Steady-state kinetics

The effect of substrate concentration on urease activity was investigated at 25 °C by varying the urea concentration from 1 mM to 30 mM at optimum pH 7.2 for soluble and immobilized enzyme. The activity assay was performed as described earlier. K_m and V_{max} were determined from a Lineweaver–Burk plot and turnover number (K_{cat}) was calculated as shown in Table 3.

2.6. Storage and stability studies of urease in nanogels

The soluble and immobilized urease were stored in 100 mM Tris-acetate-saline buffer at pH 7.2 and 4 °C. The activity was determined and recorded for four weeks at regular intervals for stored urease (immobilized and soluble) using assay procedures described in Section 2.4 on enzyme assay under similar conditions. The percent residual activity was plotted against the number of days, as shown in Fig. 7. The stability of immobilized urease enzyme in different nanogels with 90% residual enzyme activity was calculated from such a plot.

3. Results and discussion

3.1. Alginate nanogels by emulsification method

The use of self-assembled surfactant as a template is one of the most promising approaches for the synthesis of nanomaterials. The central idea of using surfactant templates is to turn the dynamic molecular aggregates into a chemically and mechanically stable supramolecular material through templating reactions. Therefore, we chose the commonly employed water-in-oil (W/O) emulsion of a nonionic surfactant for the preparation of alginate nanogels in a water-hexane biphasic system. The preparation of emulsions with droplet sizes in the 200 nm range may be performed by high energy input techniques like high-shear stirring, high-pressure homogenizers, or ultrasound generators in the presence of surfactant. In addition, the smaller the droplet size, the more energy and/or surfactant is required, making these preparation routes unfavourable for industrial applications [31]. Therefore, we chose micellar structures, which form spontaneously in organic solvents through thermodynamic self-assembly, to use as templates for alginate nanogel preparation by the sol-gel method.

Tween 80 is a nonionic surfactant selected for the present work because of its expected advantage over anionic and cationic surfactants, such as AOT (sodium bis[2-ethylhexyl] sulfosuccinate) or CTAB (cetyltrimethylammonium bromide). The behavior of anionic or cationic surfactants is strongly affected by the presence of divalent ions (Ca^{+2}, Sr^{+2}, Ba^{+2}), whereas nonionic surfactants show less pronounced interactions with these ions. Also, the presence of a

hydrophilic nonionic surfactant with a high hydrophilic-lipophilic balance (HLB) stabilizes the aqueous phase, which promotes W/O microemulsion formation. The microemulsion droplets act as nanoreactors, where the high HLB value of the nonionic surfactant promotes smaller droplet size formation, resulting in particles of smaller size due to a decrease in the sol-solvent interfacial tension [32,33].

It is also desirable to form emulsions/microemulsions with a minimum amount of surfactant. The critical micelle concentration (CMC) of surfactants for aqueous-surfactant systems has been well-studied, but few data are available for organic-surfactant systems. Hence, we applied DLS to study the emulsion in the organic phase, which allows measurement of the micelles' hydrodynamic size and provides information on the surfactant's CMC [34,35]. The results for Tween-80 in hexane are shown in Fig. 1. Each data point is averaged from three independent measurements, and the standard deviation is calculated.

The hydrodynamic diameter of Tween 80 aggregates in hexane initially increases with surfactant concentration and PDI value (0.3–0.8), then remains roughly constant at around 65 nm over a wide range of concentration. The DLS result at [Tween 80] = 7 mM is shown in Fig. 2. It confirms that Tween 80 forms stable micellar-type aggregates at concentrations of 7 mM or higher; the size is consistent with published results [36,37].

In W/O-type emulsions, at the CMC and above, the spherical micelles enclose the sol (alginate aqueous phase) in so-called water pools [38,39]. For the present sol-gel process based on emulsion polymerization, these can be called "sol pools." The size of the pool depends on the relative quantity of the aqueous phase as well as the number of surfactant molecules forming the micelles. Gelation of these sol pools in general produces spherical gel particles. Nevertheless, reasonably satisfactory alginate aqueous phase/hexane emulsions over a wide range of alginate sol volume fractions could be prepared with Tween 80 dissolved in the hexane phase. Since sodium alginate sol is insoluble in oil (hexane), the alginate polymer is confined within the aqueous nanophase. The phase stability of the resulting microemulsion is significantly affected by the amount of added alginate solution. The trial compositions were plotted on a ternary phase diagram as shown in Fig. 3A. At constant surfactant:hexane ratio for low alginate sol concentration, a transparent microemulsion region appeared. The area bounded by the square points in the phase diagram (Fig. 3A) corresponds to the

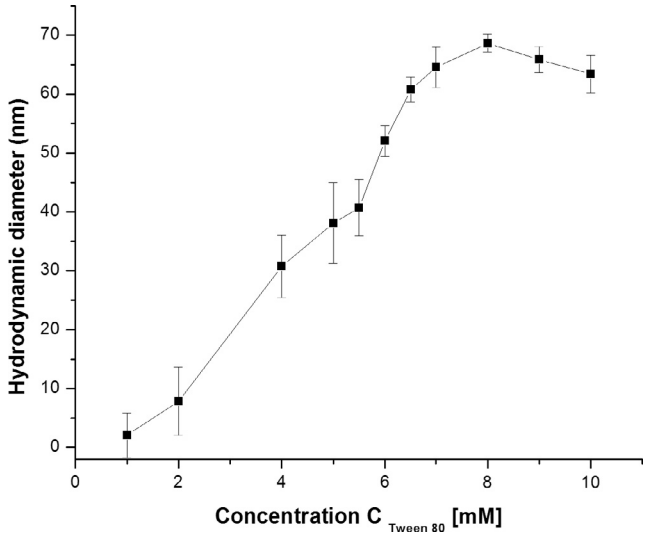

Fig. 1. Apparent hydrodynamic diameter of aggregates formed by Tween 80 in hexane measured by DLS. Error bars are standard deviations.

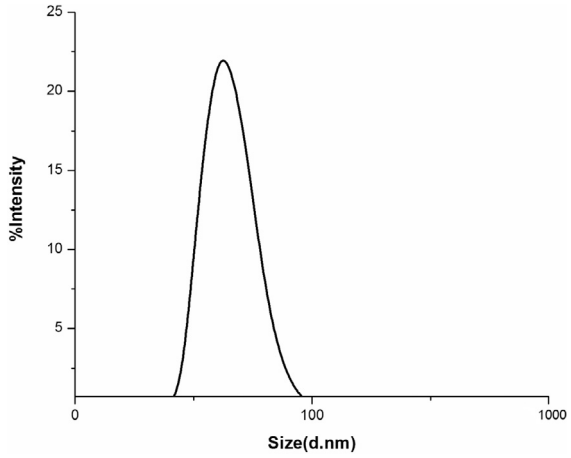

Fig. 2. Intensity based size distribution (PDI = 0.371) of micelles formed at 7 mM Tween 80 in hexane measured by DLS.

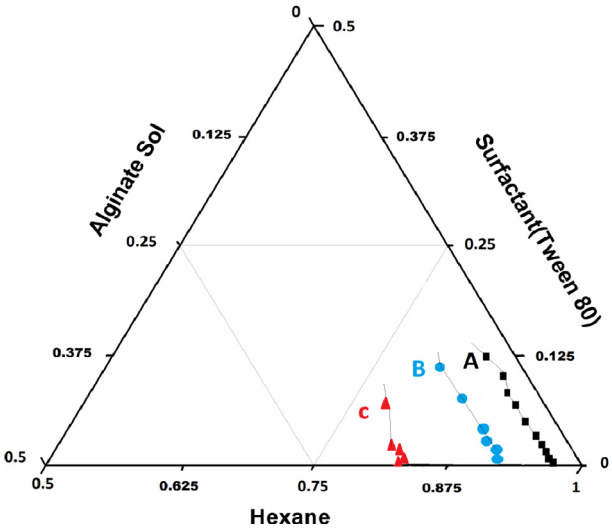

Fig. 3A. Phase diagram for a hexane/alginate solution/Tween 80 (micro)emulsion. Squares (■), circles (●) and triangles (▲) correspond to the microemulsion regions where the micelle size varies from 70 nm to 110 nm, 110 nm to 150 nm, and 160 nm to 300 nm, respectively, all with PDI less than 0.5.

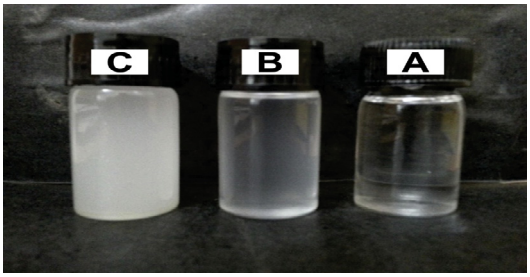

Fig. 3B. W/O microemulsion representing points A (clear solution-microemulsion), B (slightly turbid solution) and C (milky appearance-emulsion) in Fig. 3A.

concentration range of component mixtures that produced visually clear and transparent microemulsions.

The droplet size was 70 ± 3.43 (std) nm at point A in the ternary phase diagram; the corresponding microemulsion is shown in Fig. 3B. As the alginate aqueous phase concentration increases, the system becomes slightly turbid/translucent, *e.g.*, the circles in Fig. 3A, where point B represents a microemulsion with droplet

size 130 ± 10 nm. At still higher alginate, microemulsions with a milky appearance were obtained, as shown by the triangles in Fig. 3A, where at point C the droplet size is 240 ± 5.25 nm. The corresponding microemulsions at points B and C are shown in Fig. 3B.

Subsequent addition of divalent cation solutions ($CaCl_2$, $SrCl_2$, $BaCl_2$) induces gelation and leads to phase separation, which typically yields an alginate nanogel containing $Ca^{+2}/Sr^{+2}/Ba^{+2}$ as cross-linker, with a hydrodynamic diameter slightly larger than the original microemulsion droplets, as shown in Table 1. We used an alginate polymer with high mannuronate content, because this composition is more stable to NaCl treatment [10]. As a consequence of their different affinities for divalent cations, the high M-alginate nanogels obtained in the presence of Ca^{+2}, Sr^{+2} and Ba^{+2} show gradations in hydrodynamic diameter as illustrated in Table 1. The Ca-alginate nanogels are smallest and the Ba-alginate nanogels are largest, while Sr-alginate nanogels are intermediate in size. These results correlate well with earlier observations of high M-alginate capsule preparation, where a similar variation of alginate bead size was observed in microcapsule development. [12,40]. The nanophase confinement of sodium alginate polymers during emulsion polymerization does not control the gel size. The interaction of ionic polysaccharide with gelling solution leads to the formation of junction zones that may affect the hydrodynamic size of the nanogels (see Fig. 4).

3.2. SEM-EDX studies

DLS experiments provide ensemble averages of apparent particle radii. In order to get further insight into the character of our nanogels with respect to morphology and dimensions, we examined smears or films of lyophilized nanogels in ethanol by SEM. We used 0.1 M gelling solution, which is sufficient to replace all the sodium ions from the linear polymeric chain of sodium alginate. To confirm the replacement of sodium ions by divalent gelling ions, EDX spectra were recorded as shown in Figs. 5A–5C. The spectra show the relative proportion of elements present in the different nanogels and contain cation peaks for the replacement divalent cations (Ca^{+2}, Sr^{+2}, Ba^{+2}).

SEM images of the nanogels are shown as insets in Figs. 5A–5C. The spherical nanoalginate particles containing the divalent cations (Ca^{+2}, Sr^{+2}, Ba^{+2}) have much smaller diameters than the hydrodynamic diameters measured by DLS and are relatively monodisperse. The lyophilized calcium-alginate, strontium-alginate and barium-alginate nanogels had average diameters of 45.3 ± 2.4 nm, 51.4 ± 8.2 and 86.8 ± 10.6 nm, respectively, increasing with the ionic radii of the divalent cations, as was the case for the hydrodynamic diameters. Enzyme encapsulation had very little effect on the particle sizes.

3.3. FTIR spectral study

Sodium alginate (powder), lyophilized alginate nanogels containing different cations and urease-encapsulated nanogels were

Table 1
DLS data obtained from microemulsions with different divalent cation solutions collected before and 1 h after addition of divalent cation solutions.

Gelling solution (0.1 M–2 mL)	Droplet size of emulsion without aqueous phase (nm) before gelation	Recovered nanogels with cations (nm) after gelation	Shape
$CaCl_2$	70 ± 1.42 (std)	80 ± 2	Spherical
$SrCl_2$	70 ± 1.42	90 ± 5	Spherical
$BaCl_2$	70 ± 1.42	110 ± 1.4	Spherical

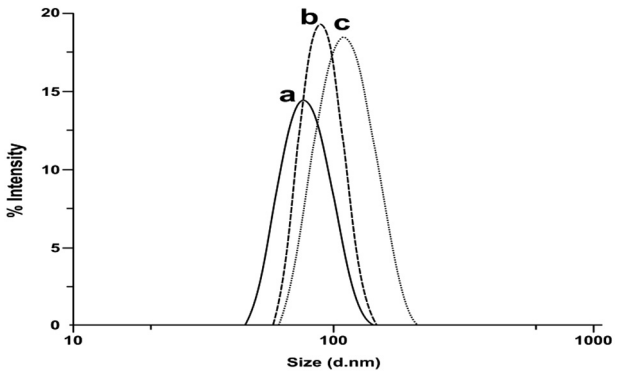

Fig. 4. Hydrodynamic diameter of alginate nanogels measured in water. (a) Ca-alginate nanogel; (b) Sr-alginate nanogel; (c) Ba-alginate nanogel.

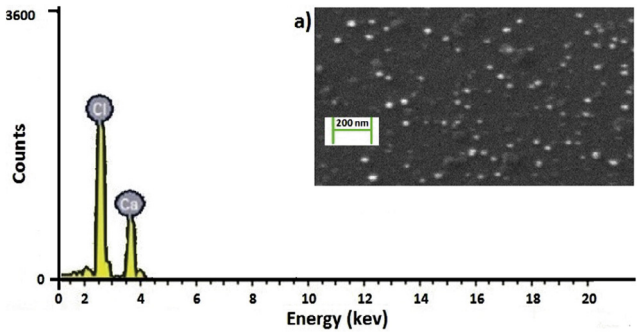

Fig. 5A. EDX spectrum of Ca-alginate nanogels showing the presence of Ca in the nanogel. Inset (a) SEM image of Ca-alginate nanogel.

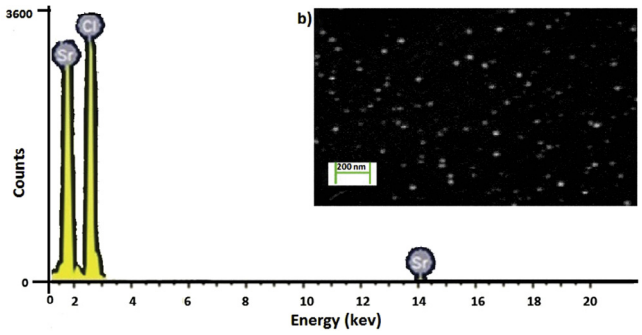

Fig. 5B. EDX spectrum of Sr-alginante nanogels showing the presence of Sr in the nanogel. Inset (b) SEM image of Sr-alginate nanogel.

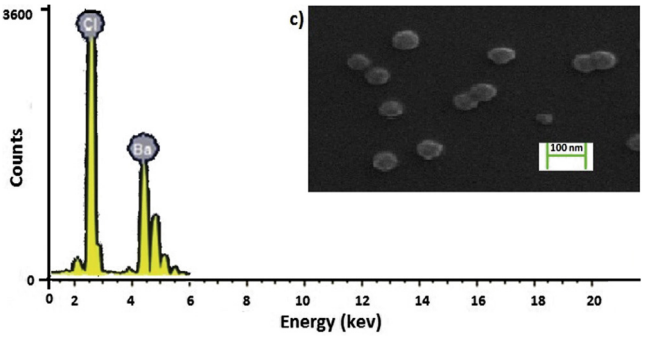

Fig. 5C. EDX spectrum of Ba-alginante nanogels showing the presence of Ba in the nanogel. Inset (c) SEM image of Ba-alginate nanogel.

analyzed using an FT-IR spectrophotometer to study cation-alginate interaction before and after gelation. The spectra of the three crosslinked alginates are quite similar. The corresponding FTIR spectra are given in the supplementary data file as Fig. 1A–1D. There are four particularly relevant spectral bands in these nanogels prepared and tested under the same conditions. The ν(O—H) (1) bands are broadened and shifted to lower wave numbers compared to linear polymeric Na-alginates, indicating that the O—H bond is weakened due to hydrogen bonding in the gel structure [41]. The ratio of intensities of ν(C=O) (2) and ν(C—OH) (3) suggests the presence of a protonated carboxylic group in the nanogels. Band (4) indicates the presence of an O-glycosidic bond between β-d-mannuronic and α-l-guluronic acid residues in the linear alginate chain. The bands in these regions are broadened and smoothed with a shift to lower wave number relative to sodium alginate.

The FTIR spectra of nanogels containing urease are shown in Figs. 6A–6D. Three absorption bands are of particular importance. The amide A Band at 3300 cm^{-1} characterizes the N—H stretch vibration; the amide I band at 1650 cm^{-1} corresponds to the C=O stretch vibration; the amide II band at 1550 cm^{-1} arises from the N—H bending vibration. C—N stretching vibrations at 1250 cm^{-1} are also prominent. We note that these infrared bands are broad and often overlap with neighboring bands to produce a complex absorption profile as shown in Figs. 6A–6D [42].

The spectra of all the crosslinked alginates are quite similar, but in the spectra of the urease-bound metal alginates, a significant new peak (5) appears at 1250 cm^{-1}, due to C—N stretching vibrations, which suggests proper encapsulation of urease in the alginate matrix.

3.4. Surface charge and physical stability (zeta potential)

The interaction of a protein with polymers and other biomaterials used in medical devices has characteristic electrical properties, such as the local electrostatic charge distribution and the electrical double layer potential, which play a significant role in defining the biological interactions, aggregation behavior and stability [43]. The zeta potential (ZP) is an indicator of the surface charge properties of a colloid or a particle in solution and depends on the surface potential and the thickness of the electric double layer. The zeta potentials of nanoparticles with charged functional groups at the surface are measured to determine their colloidal stability by coulombic repulsion [44]. The alginate nanogels were formed by electrostatic interaction between the negatively charged carboxylic groups of alginate and the positively charged divalent cations ($Ca^{+2}/Sr^{+2}/Ba^{+2}$) that form a crosslinked network containing a large fraction of water. The negative zeta potential values shown in Table 2 indicate an open and porous gel network with free carboxylic groups at the surfaces of the alginate nanogels, which

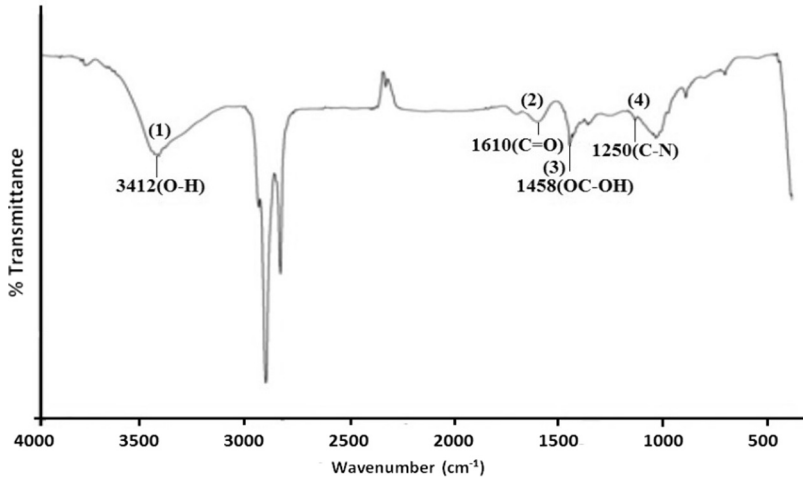

Fig. 6A. FT-IR spectrum of free urease (lyophilized powder).

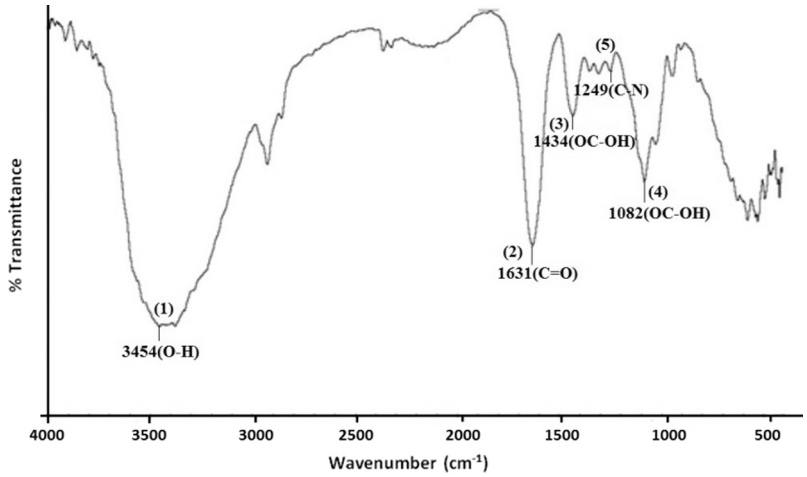

Fig. 6B. FT-IR spectrum of urease-encapsulated calcium alginate nanogel.

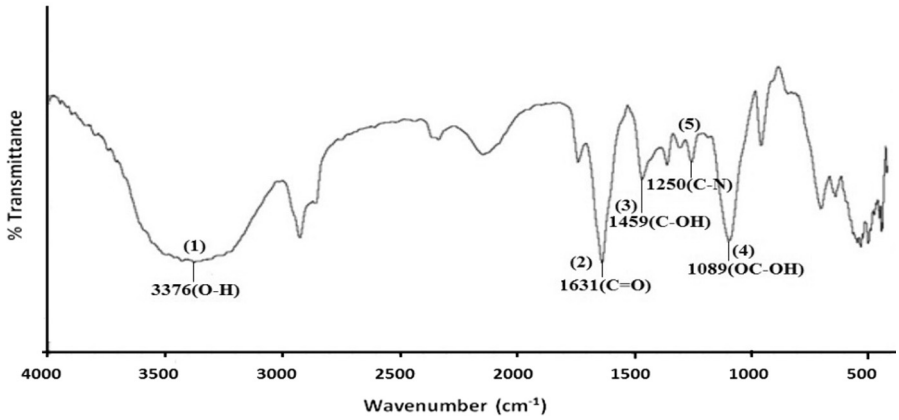

Fig. 6C. FT-IR spectrum of urease-encapsulated strontium alginate nanogel.

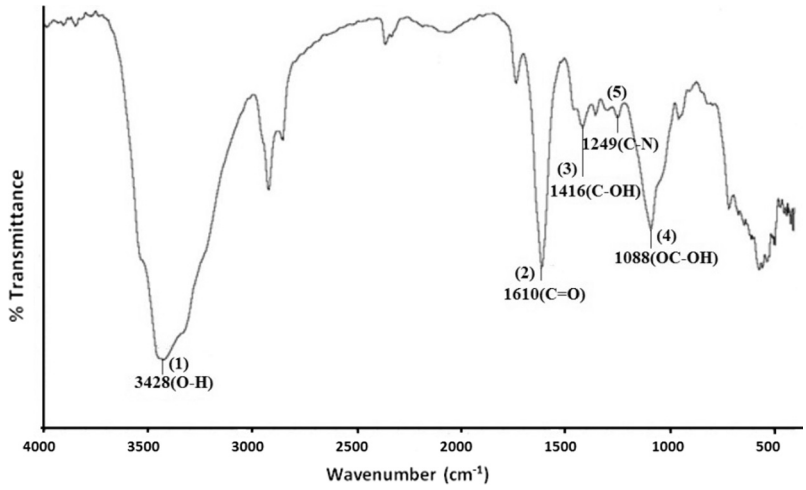

Fig. 6D. FT-IR spectrum of urease-encapsulated barium alginate nanogel.

Table 2
Zeta potentials of alginate nanogels crosslinked with divalent cations.

No.	Type of nanoparticle	Zeta potential (mV)
1.	Ca-alginate	−11.6 ± 0.2
2.	Sr-alginate	−14.8 ± 0.2
3.	Ba-alginate	−17.8 ± 0.4

causes electrostatic repulsion among the gel strands [45,46]. The high value for the Ba-alginate nanogel suggests that it has a more open gel network than the highly crosslinked Ca-alginate and Sr-alginate nanogels.

3.5. Enzyme assay

3.5.1. Steady-state kinetics

The enzymatic hydrolysis of urea can be represented by the following overall reaction [47]:

$$(NH_2)_2CO + 2H_2O \rightarrow 2NH_4^+ + CO_3^{2-} \quad (1)$$

Assuming a noncompetitive mechanism for ammonium detection using Nessler's reagent [48] leads to the following rate expression:

$$r = V_{max} \cdot [S]/(K_M + [S])(1 + [P]/K_P) \quad (2)$$

where [S] and [P] are the substrate and ammonium ion concentrations, respectively; V_{max} is the maximum reaction rate; K_m is the Michaelis-Menten constant; and K_P is the dissociation constant for the enzyme-product complex.

Kinetic data were analyzed by the initial rate method, and K_m and V_{max} values were obtained from Lineweaver-Burk plots for the three nanogels shown in Table 3. The range of concentration of urea studied was 1 mM–30 mM (~6 mg/dL to 180 mg/dL), which can be applied for measurement of blood serum urea in normal as well as kidney patients. The calibration curves were obtained for alginate gels synthesized with $BaCl_2$, $SrCl_2$ and $CaCl_2$ gelling solutions.

3.6. Storage stability of urease in nanogel

All forms of urease were stored at 4 °C in 100 mM Tris-acetate-saline buffer, pH 7.2. The storage and stability of immobilized urease in alginate nanogel crosslinked with different cations were determined by measuring the specific enzyme activity of immobilized urease and soluble urease in Tris-saline buffer at 25 °C over a period of four weeks as described in Section 2.4. The % residual activity of immobilized enzyme was compared with that of soluble enzyme, as shown in Fig. 7. Urease encapsulated in Ba-alginate nanogel was found to be active for 20 days with retention of 90% activity.

Table 3
Kinetic and stability parameters of urease enzyme.

No.	Type of alginate nano-particles	Enzyme loading efficiency (%)	Enzyme loading capacity	% immobilization	Substrate concentration effect (V_{max}) at 0.01 mg/mL urease concentration (mM/min)	K_m (mM)	Turnover no.	Linear range of calibration curve (mM)	Storage and stability with 90% activity (days)
1	Urease in Tris acetate	–	–	100	–	1.4	–	–	2
2.	Calcium alginate	64.0	0.064	83.5	1.069	0.408	59.424	2.0–24.0	10
3.	Strontium alginate	87.5	0.087	73.2	1.275	0.692	70.82	5.0–19	6
4.	Barium alginate	90.0	0.089	76.41	1.355	1.176	75.3	0.8–30	20

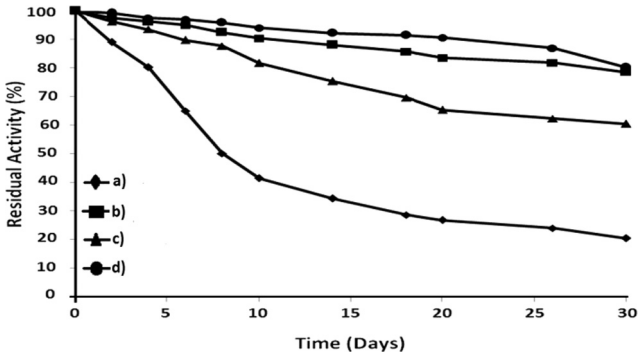

Fig. 7. Storage stability of soluble and immobilized urease at 4 °C. (a) Soluble urease in buffer; (b) encapsulated urease in Ca-alginate; (c) encapsulated urease in Sr-alginate; (d) encapsulated urease in Ba-alginate. Each experimental point represents the mean of three determinations.

3.7. Estimation of serum urea with immobilized urease

In order to determine the best matrix for urease immobilization and urea detection for clinical applications, the nanogels cross-linked with Ca^{+2}, Sr^{+2} and Ba^{+2} were tested for clinical analysis of urea in blood serum samples as reported earlier [49,50]. The clinical blood serum samples were obtained from the laboratory medicine department, All India Institute of Medical Sciences. The conditions for obtaining a constant and stable reading (amount of particle, total test volume and incubation time) were developed for a urea concentration of 180 mg/dl (~30 mM) as test analyte, which can be applied for the measurement of blood serum urea in normal humans as well as kidney patients. It is much higher than the normal physiological range (20–40 mg/dl).

The results shown in Fig. 8 indicate that urease encapsulated in Ba-alginate nanogels is most suitable for serum urea measurement, as these gels show the most reproducible response, with less than 5% relative standard deviation (RSD) within the normal physiological range of urea concentration and the high urea concentrations found in kidney patients. Ca-alginate nanogels are comparable in performance to Ba-alginate gels only at low urea. Urea detection using Sr-alginate nanogels has a very high RSD, which could be due to a low stability and detection range.

4. Conclusion

Alginate nanogels of different sizes were successfully prepared using a mild method that exploits surfactant self-assembly for templating. We have compared the effects of various gelling ions on the size and morphology of nanogels. The immobilization properties of enzyme encapsulation techniques of different nanogels were compared with respect to enzyme loading efficiency, loading capacity and turnover number. The key findings of the study are: (1) Tween 80 forms stable microemulsion droplets at 7 mM or above with hydrodynamic diameter ~65 ± 10 nm and a monomodal size distribution using a low energy emulsion technique; (2) Nanophase confinement of alginate sol by the surfactant aggregate has no controlling effect on the gel size. The size of nanogels varies with the crosslinking cation and its affinity for the mannuronate and guluronate units in the linear alginate chain; (3) The negative zeta potential indicates the presence of free carboxylic acid groups at the surface of the nanogels, leading to a negative charge at pH 7.2 and preventing aggregation of nanogels. Ba-alginate has a higher surface charge and hence better stability compared to the other nanogels; (4) In the present study, we have used sodium alginate gel of high M/G ratio, which is more stable in the presence of

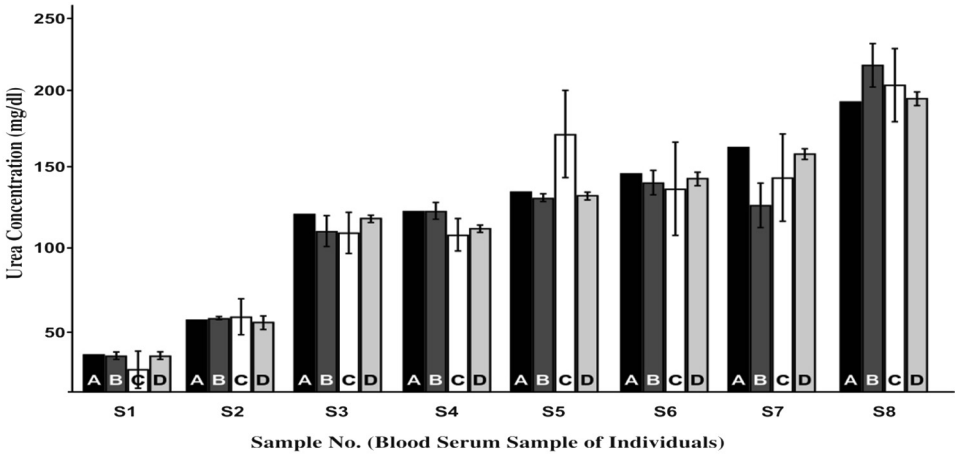

Fig. 8. Column chart showing comparison of blood urea concentration analyzed in individuals (S1-S8; shown on x-axis) and concentration of blood urea measured in mg/dL (shown on y-axis) by: (A) clinical method; (B) urease encapsulated in Ca-alginate; (C) urease encapsulated in Sr-alginate; (D) urease encapsulated in Ba-alginate. Error bars are relative standard deviations.

NaCl. Thus use of saline buffer not only prevented the aggregation of the nanogel during nanoparticle preparation but also allowed for long term stability over a four week period; (5) A comparative assay of urease shown in Table 3 demonstrates that Ba-alginate has 90% urease encapsulation efficiency with the highest turnover number and linear range of urea detection. Thus bioactivity was best retained in the protein-loaded Ba-alginate nanogel, which was able to protect and preserve protein stability during particle formulation, recovery and storage in Tris-acetate buffer.

Several kinds of nanoparticle immobilization matrices have been reported for urea detection by optical methods. Zhu et al. [51] have used a Ca-alginate matrix to develop an implantable glucose biosensor, but in order to avoid leaching of protein (glucose oxidase) and to increase shelf life, they coated the microgel with a polyelectrolyte nanofilm. Similarly, Swati, et al. [8] studied the use of a biocompatible Ca-alginate matrix for continuous measurement of urea in spent dialysates, which are unstable due to dissolution of Ca-alginate in phosphate saline solution and hence require coating with polyelectrolyte nanofilm and cresol dye. This is the first time that a Ba-alginate nanogel, which performs better than the other nanogels we synthesized, has been utilized for urea detection. Ba-alginate can encapsulate the protein/enzyme for 20 days with 90% activity, a performance far superior to that of the Ca-alginate and Sr-alginate nanogels. Due to their high surface charge, Ba-alginate colloids do not aggregate, and they have a maximum linear range of urea detection. The ease of enzyme immobilization in Ba-alginate nanogels and their storage stability makes them suitable candidates for applications in diagnostics, for BUN (blood urea nitrogen) kit development and for therapeutics.

Acknowledgement

We thank Dr. A.K. Srivastava, Laboratory of Medicine, All India Institute of Medical Science, Delhi, India, for providing us blood serum samples and their urea analysis, which allowed us to compare our results with the clinical methods. This work was supported by the Department of Biotechnology, New Delhi, India under a Bio-CARe women scientist scheme award to RS, [Grant No. BT/Bio-CARe/05/640/2011-12]. IRE was supported by U.S. National Science Foundation grant CHE-1362477.

Appendix A. Supplementary material

Supplementary data associated with this article can be found, in the online version, at http://dx.doi.org/10.1016/j.jcis.2016.11.030.

References

[1] G. Skjåk-Bræk, H. Grasdalen, H. Smidsrød, Inhomogeneous polysaccharide ionic gels, Carbohydr. Polym. 10 (1) (1989) 31–54.
[2] C.H. Goh, P.W. SiaHeng, L.W. Chan, Alginates as a useful natural polymer for microencapsulation and therapeutic applications, Carbohydr. Polym. 88 (1) (2012) 1–12.
[3] H. Zimmermann, S.G. Shirley, U. Zimmermann, Alginate-based encapsulation of cells: past, present, and future, Curr. Diab. Rep. 7 (4) (2007) 314–320.
[4] I. Ghidoni, T. Chlapanidas, M. Bucco, F. Crovato, M. Marazzi, D. Vigo, M.L. Torre, M. Faustini, Alginate cell encapsulation: new advances in reproduction and cartilage regenerative medicine, Cytotechnology 58 (1) (2008) 49–56.
[5] P. Soon-Shiong, E. Feldman, R. Nelson, R. Heintz, Q. Yao, Z. Yao, T. Zheng, N. Merideth, G. Skjak-Braek, T. Espevik, Long-term reversal of diabetes by the injection of immunoprotected islets, Proc. Natl. Acad. Sci. USA 90 (12) (1993) 5843–5847.
[6] S. Mizrahy, D. Peer, Polysaccharides as building blocks for nanotherapeutics, Chem. Soc. Rev. 41 (7) (2012) 2623–2640.
[7] P. Agulhon, M. Robitzer, L. David, F. Quignard, Structural regime identification in ionotropic alginate gels: influence of the cation nature and alginate structure, Biomacromolecules 13 (1) (2012) 215–220.
[8] M. Swati, N.K. Hase, R. Sivastava, Nanoengineered optical urea biosensor for estimating haemodialysis parameters in spent dialysate, Anal. Chim. Acta 676 (1–2) (2010) 68–74.
[9] A. Chaudhary, M. Raina, H. Harma, P. Hanninen, M.J. McShane, R. Srivastava, Evaluation of glucose sensitive affinity binding assay entrapped in fluorescent dissolved-core alginate microspheres, Biotechnol. Bioeng. 104 (6) (2009) 1075–1085.
[10] O. Smidsrod, G. Skjak-Braek, Alginate as immobilization matrix for cells, Trends Biotechnol. 8 (3) (1990) 71–78.
[11] K.Y. Lee, D.J. Mooney, Alginate: properties and biomedical applications, Prog. Polym. Sci. 37 (1) (2012) 106–126.
[12] Y.A. Mørch, I. Donati, B.L. Strand, G. Skjåk-Braek, Effect of Ca^{2+}, Ba^{2+}, and Sr^{2+} on alginate microbeads, Biomacromolecules 7 (5) (2006) 1471–1480.
[13] E. Callone, R. Campostrini, G. Carturan, A. Cavazza, R. Guzzon, Immobilization of yeast and bacteria cells in alginate microbeads coated with silica membranes: procedures, physico-chemical features and bioactivity, J. Mater. Chem. 18 (40) (2008) 4839–4848.
[14] T. Coradin, N. Nassif, J. Livage, Silica–alginate composites for microencapsulation, Appl. Microbiol. Biotechnol. 61 (5) (2003) 429–434.
[15] F. Kurayama, S. Suzuki, N.M. Bahadur, T. Furusawa, H. Ota, M. Sato, N. Noboru Suzuki, Preparation of aminosilane-alginate hybrid microcapsules and their use for enzyme encapsulation, J. Mater. Chem. 22 (30) (2012) 15405–15411.
[16] J.P. Paques, E. van der Linden, C.J. van Rijn, L.M. Sagis, Preparation methods of alginate nanoparticles, Adv. Colloid Interface Sci. 209 (2014) 163–171.
[17] M. Rajaonarivony, C. Vauthier, G. Couarraze, F. Puisieux, P. Couvreur, Development of new drug carrier made from alginate, J. Pharm. Sci. 82 (9) (1993) 912–917.
[18] C. Yu, H. Wei, Q. Zhang, X. Zhang, S. Cheng, R. Zhuo, Effect of ions on the aggregation behavior of natural polymer alginate, J. Phys. Chem. B 113 (45) (2009) 14839–14843.
[19] C.P. Reis, R.J. Neufeld, A.J. Ribeiro, F. Veiga, Nanoencapsulation I. Methods for preparation of drug-loaded polymeric nanoparticles, Nanomedicine 2 (1) (2006) 8–21.
[20] C.P. Reis, R.J. Neufeld, S. Vilela, A.J. Ribeiro, F. Veiga, Review and current status of emulsion/dispersion technology using an internal gelation process for the design of alginate particles, J. Microencapsul. 23 (3) (2006) 245–257.
[21] A.H. Machado, D. Lundberg, A.J. Ribeiro, F.J. Veiga, B. Lindman, M.G. Miguel, U. Olsson, Preparation of calcium alginate nanoparticles using water-in-oil (W/O) nanoemulsions, Langmuir 28 (9) (2012) 4131–4141.
[22] M. Zhybak, V. Beni, M.Y. Vagin, E. Dempsey, A.P.F. Turner, Y. Korpan, Creatinine and urea biosensors based on a novel ammonium ion-selective copper-polyaniline nano-composite, Biosens. Bioelectron. 77 (2016) 505–511.
[23] J. Emsley, Molecules at an Exhibition: Portraits of Intriguing Materials in Everyday Life, Oxford University Press, Oxford, 1999, p. 200.
[24] G.K. Mishra, R.K. Mishra, S. Bhand, Flow injection analysis biosensor for urea analysis in adulterated milk using enzyme thermistor, Biosens. Bioelectron. 26 (4) (2010) 1560–1564.
[25] S. Andreescu, J. Njagi, C. Ispas, Nanostructured materials for enzyme immobilization and biosensors – Chapter 7, New Front. Organ. Compos. Nanotechnol. (2008) 355–394.
[26] S. Datta, L.R. Christena, Y.R.S. Rajaram, Enzyme immobilization: an overview on techniques and support materials, Biotechnology 3 (1) (2013) 1–9.
[27] J.C.W. Corbett, F. McNeil-Watson, R.O. Jack, M. Howarth, Measuring surface zeta potential using phase analysis light scattering in a simple dip cell arrangement, Colloids Surf. A: Physicochem. Eng. Asp. 396 (2012) 169–176.
[28] S. Kumar, A. Dwevedi, A.M. Kayastha, Immobilization of soybean (Glycine max)urease on alginate and chitosan beads showing improved stability: analytical applications, J. Mol. Catal. B: Enzym. 58 (1–4) (2009) 138–145.
[29] L.H. Pignolet, A.S. Waldman, L. Schechinger, G. Govindarajoo, J.S. Nowick, The alginate demonstration: polymers, food science, and ion exchange, J. Chem. Educ. 75 (11) (1998) 1430.
[30] M.M. Bradford, A rapid and sensitive method for the quantitation of microgram quantities of protein utilizing the principle of protein-dye binding, Analyt. Biochem. 72 (1976) 248–254.
[31] M. Porras, C. Solans, C. González, J.M. Gutiérrez, Properties of water-in-oil(W/O) nanoemulsions prepared by a low energy emulsification method, Colloids Surf. A: Physicochem. Eng. Asp. 324 (1–3) (2008) 181–188.
[32] B. Siladitya, M. Chatterjee, D. Ganguli, Role of organic solvents and surface active agents in the sol emulsion gel synthesis of spherical alumina powders, J. Mater. Res. 15 (1) (2000) 176–185.
[33] E. Dickinson, Chapter 7 – emulsions and droplet size control, in: D.J. Wedlock (Ed.), Controlled Particle, Droplet and Bubble Formation, Butterworth-Heinemann, 1994, pp. 191–216.
[34] B.J. Berne, R. Pecora, Dynamic Light Scattering: With Applications to Chemistry, Biology, and Physics, 1976 edition., John Wiley & Sons Inc., New York, 1976.
[35] M. Zulauf, H. Friedrich, Eicke, Inverted micelles and microemulsions in the ternary system water/aerosolOT/isooctane as studied by photon correlation spectroscopy, J. Phys. Chem. 83 (4) (1979) 480–486.
[36] R.K.O. Apenten, Q.H. Zhu, Interfacial parameters for selected spans and Tweens at the hydrocarbon-water interface, Food Hydrocolloids 10 (1) (1996) 27–30.
[37] R. Davies, D.E. Graham, B. Vincent, Water cyclohexane "Span 80" "Tween 80" systems: Solution properties and water/oil emulsion formation, J. Colloid. Interface Sci. 116 (1) (1987) 88–99.
[38] M. Yoshida, M. Lal, N.D. Kumar, P.N. Prasad, TiO_2 nanoparticle dispersed polyimide composite optical wave guide materials through reverse micelles, J. Mater. Sci. 32 (15) (1997) 4047–4051.

[39] A. Aryal, L. Cot, T. Dabadie, C. Guizard, J. Ramsay, SANS investigations of oxide gel formation in inverse micelle and lamellar surfactant systems, J. Sol-Gel Sci. Technol. 2 (1) (1994) 205–209.
[40] B.L. Strand, O. Gåserød, B. Kulseng, T. Espevik, G. Skjåk-Baek, Alginate-polylysine-alginate microcapsules: effect of size reduction on capsule properties, J. Microencapsulation 19 (5) (2002) 615–630.
[41] E. Torres, Y.N. Mata, M.L. Blázquez, J.A. Muñoz, F. González, A. Ballester, Gold and silver uptake and nanoprecipitation on calcium alginate beads, Langmuir 21 (17) (2005) 7951–7958.
[42] C.R. Cantor, P.R. Schimmel, Techniques for the study of biological structure and function, Biophysical Chemistry: Part II, WH Freeman and Co., Oxford, 1980, p. 503.
[43] S.A.M. Tofail (Ed.), Biological Interactions With Surface Charge in Biomaterials, RSC Publishing, 2011. ISBN 978-1-84973-185-0.
[44] R.J. Hunter, Zeta Potential in Colloid Science: Principles and Publications, Academic Press, London; New York, 1981.
[45] O. Gaseroed, O. Smidsroed, G. Skjak-Braek, Microcapsules of alginate-chitosan—I: A quantitative study of the interaction between alginate and chitosan, Biomaterials 19 (20) (1998) 1815–1825.
[46] H.G. Xie, J.N. Zheng, X.X. Li, X.D. Liu, J. Zhu, F. Wang, W.Y. Xie, X.J. Ma, Effect of surface morphology and charge on the amount and conformation of fibrinogen adsorbed onto alginate/chitosan microcapsules, Langmuir 26 (8) (2010) 5587–5594.
[47] M. Fidaleo, R. Lavecchia, Kinetic study of enzymatic urea hydrolysis in the pH range 4–9, Chem. Biochem. Eng. Q. 17 (4) (2003) 311–318.
[48] J.P. Hoare, K.J. Laidler, The molecular kinetics of the urea-urease system. II. The inhibition by products, J. Am. Chem. Soc. 72 (6) (1950) 2487–2489.
[49] R. Sahney, S. Anand, B.K. Puri, A.K. Srivastava, Immobilization of urease on glass pH electrodes: A comparative study between three immobilization techniques and its application in urea detection in blood serum, Anal. Chim. Acta 578 (2006) 156–161.
[50] R. Sahney, S. Anand, B.K. Puri, Enzyme coated glass pH-electrode: Its fabrication and application in the determination of urea in blood samples, Anal. Chim. Acta 542 (2005) 157–161.
[51] H. Zhu, R. Srivastava, J.Q. Brown, M.J. McShane, Combined physical and chemical immobilization of glucose oxidase in alginate microspheres improves stability of encapsulation and activity, Bioconjugate Chem. 16 (6) (2005) 1451–1458.